9448 *Biochemistry* **2009,** *48,* 9448–9455
DOI: 10.1021/bi900279x

BIOCHEMISTRY
including biophysical chemistry & molecular biology
Article

Functional Energetic Landscape in the Allosteric Regulation of Muscle Pyruvate Kinase. 1. Calorimetric Study[†]

Petr Herman*[,‡,§] and J. Ching Lee*[,§]

[‡]*Faculty of Mathematics and Physics, Institute of Physics, Charles University, Ke Karlovu 5, 121 16 Prague, Czech Republic, and* [§]*Department of Biochemistry and Molecular Biology, University of Texas Medical Branch, Galveston, Texas 77555-1055*

Received February 18, 2009; Revised Manuscript Received July 23, 2009

ABSTRACT: Rabbit muscle pyruvate kinase (RMPK) is an important allosteric enzyme of the glycolytic pathway catalyzing a transfer of the phosphate from phosphoenolpyruvate (PEP) to ADP. The energetic landscape of the allosteric regulatory mechanism of RMPK was characterized by isothermal titration calorimetry (ITC) in the temperature range from 4 to 45 °C. ITC data for RMPK binding to substrates PEP and ADP, for the allosteric inhibitor Phe, and for combination of ADP and Phe were globally analyzed. The thermodynamic parameters characterizing the linked-multiple-equilibrium system were extracted. Four novel insights were uncovered. (1) The binding preference of ADP for either the T or R state is temperature-dependent, namely, more favorable to the T and R states at high and low temperatures, respectively. This crossover of affinity toward R and T states implies that ADP plays a complex role in modulating the allosteric behavior of RMPK. Depending on the temperature, binding of ADP can regulate RMPK activity by favoring the enzyme to either the R or T state. (2) The binding of Phe is negatively coupled to that of ADP; i.e., Phe and ADP prefer not to bind to the same subunit of RMPK. (3) The release or absorption of protons linked to the various equilibria is specific to the particular reaction. As a consequence, pH will exert a complex effect on these linked equilibria, resulting in the proton being an allosteric regulatory ligand of RMPK. (4) The R ↔ T equilibrium is accompanied by a significant ΔC_p, rendering RMPK most sensitive to temperature under physiological conditions. During muscle activity, both pH and temperature fluctuations are known to happen; thus, results of this study are physiologically relevant.

A serious challenge of the postgenomic era is to establish the correlation between protein structural folds and functions. With knowledge of the protein sequence through the genomic data, a popular practice is to employ various types of algorithms to model the structural fold as defined by the protein sequence. However, it is soon recognized that diverse functions are carried out by proteins with essentially identical folds but different sequences. Many protein structural folds have been identified, e.g., the various folds involved in signal transduction (*1*−*3*). The chemical principles that govern the relation between function and sequence differences within a fold are still unclear.

We have chosen the biological phenomenon of allosteric regulation as the focus to tackle the issue of sequence−function correlation. The rationale for the choice is that allostery is a predominant regulatory mechanism and an allosteric system consists of a variety of functions that can be modulated by a change in sequence.

Rabbit muscle pyruvate kinase (RMPK) is an ideal system that has an outstanding chance of revealing the chemical principles of allostery. The unique feature that makes RMPK an ideal system is that PK exists in four isozymic forms (*4*, *5*). Between two of these isozymes, only 22 amino acid changes in 530 residues per subunit are required to convert an enzyme with a classical Michealis−Menten activity profile to one with distinct sigmoidal activity profiles. Thus, imbedded in these two isoforms of PK is information for relating the change in protein sequence to functional changes. Furthermore, no significant structural changes in RMPK are associated with these changes in residues (*4*, *5*).

RMPK is an important allosteric enzyme of the glycolytic pathway catalyzing a transfer of the phosphate from phosphoenolpyruvate (PEP) to ADP (*6*−*10*):

$$\mathrm{PEP} + \mathrm{ADP} \overset{\mathrm{PK}}{\leftrightarrow} \mathrm{pyruvate} + \mathrm{ATP}$$

Production of ATP is essential in the cell energetics, and therefore, it is not surprising that RMPK activity is subjected to an intriguing pattern of regulation. RMPK consists of four identical subunits (*11*). Its activity is regulated by metabolites. Besides the two substrates, PEP and ADP, the enzyme also requires Mg^{2+} and K^+ for its activity (*12*). RMPK was found to be allosterically inhibited by L-phenylalanine (Phe) (*13*). Although the in vivo significance of this allosteric inhibitor is not fully understood yet, its effect on enzyme kinetics and related conformational changes were well-documented in both structural data (*14*−*17*) and steady state enzyme kinetics (*8*, *10*, *14*−*21*). It was shown that steady state kinetic data follow a simple hyperbolic Michaelis−Menten equation in the absence of Phe. However, the steady state kinetic behavior exhibits increasing sigmoidicity in the presence of increasing Phe concentrations. Phe binding was found to induce a highly cooperative conformation change as monitored by sedimentation techniques (*18*), analytical gel-filtration chromatography (*22*), and small-angle neutron

[†]Supported by National Institutes of Health Grant GM 77551 and the Robert A. Welch Foundation (J.C.L.) and Grant MSM 0021620835 from the Ministry of Education, Youth and Sports of the Czech Republic (P.H.).

*To whom correspondence should be addressed. J.C.L.: telephone, (409) 772-2281; fax, (409) 772-4298; e-mail, jclee@utmb.edu. P.H.: telephone, +420-221911461; fax, +420-224922797; e-mail, herman@karlov.mff.cuni.cz.

 Published on Web 08/31/2009

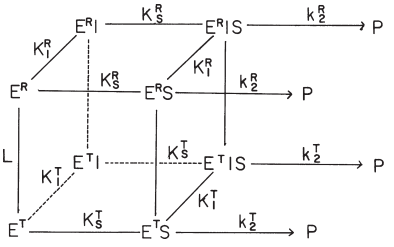

FIGURE 1: Proposed two-state model for the allosteric behavior of RMPK.

scattering (*21*). In particular, binding of Phe to one of the four equivalent subunits causes all subunits to change conformation in a concerted manner.

Thorough analysis of the experimental evidence (*8*, *10*, *18*, *19*) suggested that all data can be consistently described by a concerted allosteric model (*23*) in which protein assumes an active (R) and an inactive (T) form with differential affinities for ligands, as shown in Figure 1. Without significant interconversion of the secondary structure during the R ↔ T transition, the two forms of the enzyme differ in hydrodynamic properties as well as in their flexibility and internal dynamics (*24*). In particular, the R state is characterized by a compact symmetric conformation of the enzyme and the T state assumes an expanded form with a significantly loosened structure. Therefore, it is not surprising that ligands may exhibit different affinities for the R and T states, and consequently, they perturb the equilibrium between these states by shifting it to one form or the other. Fourier-transformed infrared (FT-IR) experiments probing the RMPK protein dynamics by H ↔ D exchange suggested that the allosteric regulation of the enzyme is a consequence of perturbation of the distribution of states in which the R and T states represent the two extreme end states (*24*). On the basis of the results of steady state kinetic and other spectroscopic or hydrodynamic measurements, the substrate PEP and the allosteric inhibitor Phe were reported to bind preferentially to the R and T states, respectively (*8*, *10*, *21*, *22*, *24*). The second substrate, ADP, was found to bind to both states with approximately the same affinity at 23 °C (*19*).

Despite the apparent simplicity of the two-state model, full quantitative thermodynamic characterization of PK regulatory properties has yet to be attempted. A closer examination of the reactions involved in modulating RMPK activity shows that the minimum number of metabolites that interact with RMPK is four, namely, two substrates (PEP and ADP), one inhibitor (Phe), and one activator (FBP). The number of reactions linking all these metabolites interacting with the two conformation states of RMPK increases exponentially. Obviously, in the presence of multiple ligands, such as in an in vivo cellular environment, the simple two-state R ↔ T equilibrium model explodes into a highly intricate model involving simultaneous, multiple equilibria that are rather difficult to quantitatively characterize without an in-depth dissection. Though very useful, steady state enzyme kinetics suffer because of an inherent limitation that two substrates, PEP and ADP, have to be always present simultaneously in the reaction mix to induce RMPK activity. Moreover, thermodynamic coupling between ligands cannot be avoided. Since information that can be extracted from the data is always limited, published kinetic data offer only a partial characterization of the RMPK behavior.

A major assumption of our two-state model is that the binding of ligands is state-dependent; e.g., the binding constant for binding of Phe to either the R or T state is defined by the state only (namely, $K^{R}_{Phe} = K^{R}_{ADP,Phe}$ even if ADP is bound as long as PK is in the R state). In this study, we test the validity of this assumption for the Phe/ADP pair.

In this work, we focus on a thermodynamic characterization of the allosteric regulatory behavior of RMPK by isothermal titration calorimetry (ITC). ITC experiments allow direct access to fundamental thermodynamic parameters associated with ligand binding and RMPK conformational transitions. Since ITC experiments are not based on an enzymatic activity, binding of single ligands can be assessed and interaction between ligands investigated. A detailed description of the regulatory behavior of wild-type RMPK is essential for modeling its regulation under physiological conditions. It also creates an essential baseline for understanding perturbations induced by targeted genetic modifications of the recombinant enzyme.

MATERIALS AND METHODS

Materials. RMPK, phosphoenolpyruvate (PEP), and ADP were purchased from Boeringer-Manheim. Trizma base, Bis-Tris, Phe, and KCl were from Sigma, and $MgSO_4$ was from Fisher. The purity of the protein was monitored by SDS gel electrophoresis.

Methods. TKM or BTKM buffers at pH 7.5 contained 50 mM Trizma base or Bis-Tris, respectively, 72 mM KCL, and 7.2 mM $MgSO_4$. A correction for the temperature coefficients of the buffers was applied at every experimental temperature.

Ammonium sulfate precipitates of RMPK were centrifuged; the pellet was resuspended in a desired buffer and exhaustively dialyzed. The concentration of RMPK was adjusted using an absorptivity of 0.54 mg mL^{-1} cm^{-1} at 280 nm (*12*) and a molecular mass of 220 kDa (*8*). A single batch of protein was used for all experiments.

Isothermal Titration Calorimetry (*ITC*). Calorimetric titrations were performed on the Omega microcalorimeter (MicroCal, Inc.). Concentrations of RMPK ranged from 15 to 70 μM. Stock solutions of 40 mM PEP, 100 mM Phe, and 100 mM ADP were used for injections. The titrants were prepared by dilution of the ligands in the dialyzate to prevent thermal effects caused by a buffer mismatch. The pH of the titrants was checked and adjusted, if necessary. When RMPK was titrated with Phe in the presence of a fixed concentration of ADP, the same concentration of ADP was present in the injectant. Typically, 15−25 aliquots of ligand were injected into a 1.4 mL sample. To correct data for heats of dilution of an injectant, a control experiment was performed under the same conditions except a buffer was substituted for the sample. The overall reaction heats were calculated by integration of the corrected ITC curves.

The extent of irreversible processes caused by mixing of the protein at high temperatures in the calorimeter was also evaluated. Only an insignificant decrease of 3 ± 3% activity was observed after a 1 h calorimetric experiment at 40 °C.

Global Fitting. Multiple data sets were simultaneously analyzed by a global fitting routine described in detail by Knutson et al. (*25*, *26*). The global analysis is an extension of an ordinary nonlinear least-squares fitting (*27*) for simultaneous analysis of multiple experimental data sets using a single model that encompasses them all. Experiments were performed under a variety of conditions. The most important feature of the approach is that some parameters are inherently common for the different but related curves. Then the global fitting exploits

relationships between these curves and overdetermines these parameters. Such overdetermination helps both in distinguishing between competing models and in the recovery of these parameters. During the global fitting, the overall sum of weighted squared deviations of calculated values from the measured data (χ^2) is minimized to yield model parameters that are consistent with all data curves simultaneously. This approach was proven to be highly robust and was shown to maximize information that can be retrieved from the analyzed data (*28*−*34*). An in-house program utilizing the Marquardt−Levenberg minimization procedure (*35*) was used for the global analysis of the calorimetry data.

RESULTS

Description of the Model. On the basis of the published thermodynamic and steady state kinetic results from this laboratory, a model is developed. It is based on a simple, yet very versatile, model for the cooperative binding of ligands by macromolecules described by Monod et al. (*23*) and elaborated for the tertameric RMPK by Oberfelder et al. (*8*), as shown in Figure 1. For any single ligand, the two-state Monod−Wyman−Changeux (MWC) model can be described by the following scheme:

$$\begin{array}{ccccccc} & & & & L_0 & & \\ Ligand & + & R & \leftrightarrows & T & + & Ligand \\ & & \updownarrow & & \updownarrow & & \\ & & R(liganded) & \leftrightarrows & T(liganded) & & \end{array}$$

According to this model, an overall reaction heat Q_{tot} accompanying saturation of the enzyme by a ligand can be treated as a composite heat of three major reactions: heats Q^{R}_{lig} and Q^{T}_{lig} of ligand binding to the R and T states, respectively, and heat $Q_{R\leftrightarrow T}$ accompanying the R ↔ T equilibrium:

$$Q_{tot} = {}^{sat}f^{R}_{lig}Q^{R}_{lig} + {}^{sat}f^{T}_{lig}Q^{T}_{lig} + ({}^{sat}f^{T}_{lig} - f^{T}_{0})Q_{R\leftrightarrow T} \quad (1)$$

Terms ${}^{sat}f^{R}_{lig}$ and ${}^{sat}f^{T}_{lig}$ are fractions of RMPK in the R and T states, respectively, at the end of the titration when the enzyme is fully saturated by the ligand. The term f^{T}_{0} is a fraction of the unliganded T state at the beginning of the experiment.

The R ↔ T transition can be accompanied by protonation or deprotonation of the enzyme. Heat contributions from such linked proton absorptions may be expressed as follows:

$$Q^{state}_{lig} = 4M_0V_0(\Delta H^{state}_{lig} + \Delta n^{state}_{lig}\Delta H_{ion}) \quad (2)$$

$$Q_{R\leftrightarrow T} = M_0V_0(\Delta H_{R\leftrightarrow T} + \Delta n_{R\leftrightarrow T}\Delta H_{ion}) \quad (3)$$

where M_0 stands for the molar concentration of RMPK, V_0 is a sample volume, ΔH_{ion} is the ionization enthalpy of the buffer, and Δn^{state}_{lig} and $\Delta n_{R\leftrightarrow T}$ are changes in the molar amount of protons as ligand binds to the R or T state and as RMPK undergoes the R ↔ T transition, respectively. A positive or negative value for Δn indicates an absorption or release of proton, respectively. The enthalpies ΔH^{state}_{lig} and $\Delta H_{R\leftrightarrow T}$ are calculated per mole of binding sites and per mole of tetrameric RMPK, respectively.

In the two-state model, the equilibrium constant L_0 between the unliganded R and T states is characterized by the ratio

$$L_0 = \frac{[T_0]}{[R_0]} \quad (4)$$

where $[T_0]$ and $[R_0]$ are equilibrium concentrations of the unliganded T and R states, respectively. Then, the fraction (f^{T}_{0}) of the unliganded RMPK in the T state can be expressed as

$$f^{T}_{0} = L_0/(1 + L_0) \quad (5)$$

and

$$f^{T}_{0} + f^{R}_{0} = 1 \quad (6)$$

Results of the steady state kinetic measurements (*10*) as well as the recent fluorescence data (DOI: 10.1021/bi900280u) indicate that within the temperature range from 5 to 40 °C a saturating concentration of PEP or Phe shifts the RMPK population completely to the R or T state, respectively. As a consequence, eq 1 is substantially simplified because ${}^{sat}f^{R}_{Phe} = {}^{sat}f^{T}_{PEP} = 0$ and ${}^{sat}f^{R}_{PEP} = {}^{sat}f^{T}_{Phe} = 1$. Under these conditions, one can see from eqs 1−3 that experiments at ligand saturation yield information about the binding enthalpies only, and the information about entropy toward the equilibrium binding constant is lost because there is no change in state.

It was shown by steady state enzyme kinetics that at room temperature ADP exhibits only negligible differential affinity for the R and T states (*19*). When RMPK is titrated with ADP, the full eq 1 should be used for the analysis of the ITC data because only minor shifts of the R ↔ T equilibrium are expected. When RMPK is titrated with Phe in the presence of a fixed concentration of ADP, the apparent R ↔ T equilibrium constants ${}^{nonsat}L_{0,ADP} = [T_{ADP}]/[R_{ADP}]$ and ${}^{nonsat,sat}L_{0,ADP,Phe} = [T_{ADP,Phe}]/[R_{ADP,Phe}]$ at the beginning and end of the Phe titration, respectively, could differ from the ones in the absence of ADP, and these new constants should be used for calculation of the corresponding fractions ${}^{nonsat}f^{T}_{ADP}$ and ${}^{nonsat,sat}f^{T}_{ADP,Phe}$ in eq 1. On the basis of the WMC model adopted for the tetrameric enzyme (*8*), the new equilibrium constants between the R and T states in the presence of an arbitrary concentration of ADP can be expressed for tetrameric RMPK as

$$\begin{aligned} {}^{nonsat}L_{0,ADP} &= L_0\left(\frac{1 + [ADP]/K^{T}_{ADP}}{1 + [ADP]/K^{R}_{ADP}}\right)^4 {}^{nonsat,sat}L_{0,ADP,Phe} \\ &= {}^{nonsat}L_{0,ADP}\left(\frac{K^{R}_{Phe}}{K^{T}_{Phe}}\right)^4 \end{aligned} \quad (7)$$

where K^{state}_{ligand} is a microscopic dissociation constant. Moreover, an additional differential heat ΔQ_{eq} resulting from the re-equilibration of ADP between the R and T states after an addition of Phe should be added to eq 1:

$$\begin{aligned} \Delta Q_{eq} = 4M_0V_0({}^{nonsat,sat}f^{T}_{ADP,Phe} - {}^{nonsat}f^{T}_{ADP,0})[Y^{T}_{ADP}(\Delta H^{T}_{ADP} \\ + \Delta n^{T}_{ADP}\Delta H_{ion}) - Y^{R}_{ADP}(\Delta H^{R}_{ADP} + \Delta n^{R}_{ADP}\Delta H_{ion}) \end{aligned} \quad (8)$$

Y^{R}_{ADP} is the fractional saturation of the ADP binding site in the RMPK monomer:

$$Y^{state}_{ADP} = \frac{[ADP]/K^{state}_{ADP}}{1 + [ADP]/K^{state}_{ADP}} \quad (9)$$

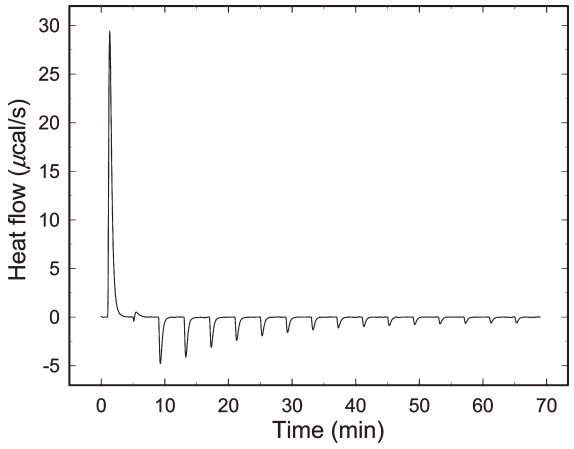

FIGURE 2: ITC curve of RMPK titrated with Phe at 38 °C.

For the global analysis, experiments performed at different temperatures can be linked together by a temperature dependence of the involved equilibrium constants:

$$-RT \times \ln(L_0) = \Delta H_{R\leftrightarrow T} - T\Delta S_{R\leftrightarrow T} \quad (10)$$

$$RT \times \ln(K_{lig}^{state}) = \Delta H_{lig}^{state} - T\Delta S_{lig}^{state} \quad (11)$$

Isothermal Titration Calorimetry (*ITC*). To establish the energetic landscape of the regulatory behavior of RMPK in the presence of its ligands, we performed a series of ITC experiments at temperatures between 4 and 45 °C. To separate the contribution of the buffer ionization heat ΔH_{ion} from the overall reaction heat, we performed all titrations in two buffers with different ΔH_{ion} values. Typically, two experiments were performed in each buffer system, and the data were averaged.

Figure 2 presents one example of the ITC titration curve, titration by Phe at 38 °C. The sign of heat exchange for the reaction changes from positive to negative during the titration. This is a clear indication that the reaction is complex and consists of at least two heat-generating processes with opposite signs. Actually, many reactions may contribute to the shape of ITC curves. The observation is consistent with the general mechanism of the WMC model which includes binding to both enzyme states, a ligand-induced shift of the R ↔ T equilibrium accompanied by the change in the RMPK conformation, and linked proton reactions as described in our model. Heats resulting from re-equilibration of ligands between the R and T states upon perturbation of the R ↔ T equilibrium contribute to the detailed shape of the titration curves as well.

Since the patterns of the ITC data are quite complex, the consequence of linked multiple equilibria, a detailed interpretation of such curves is rather difficult. Therefore, we decided not to draw conclusions only on the basis of the shape of the ITC curves. Instead, at different temperatures, we titrated RMPK to saturation, and the data are expressed as overall reaction heats. Each data point in Figures 3−6 therefore represents at least one ITC experiment.

(*i*) *PEP Binding*. ITC titrations with PEP are shown in Figure 3 which shows that the measured reaction heats exhibit a pronounced dependence on temperature. In this titration, there are only two linked reactions, namely, PEP binding and RMPK conformation change. At low temperatures of < 30 °C, the magnitude of the heat of reaction is a linear function of temperature with a small negative slope. Such a behavior reflects

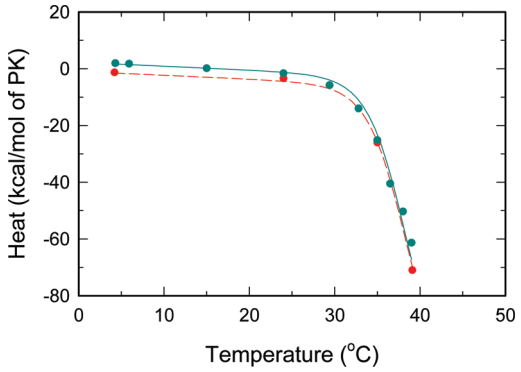

FIGURE 3: Temperature dependence of overall reaction heats for RMPK titrated with PEP. Cyan and red symbols represent data from ITC titrations in TKM and BTKM buffer, respectively. Lines represent the best global fits of all ITC data, i.e., all data from Figures 2−5.

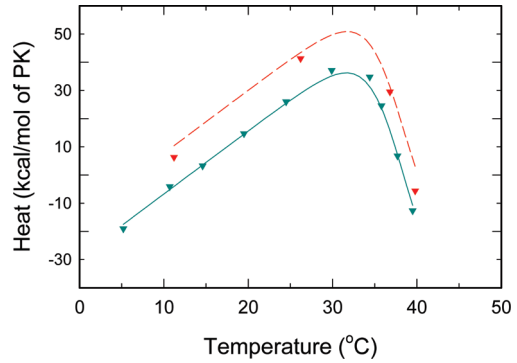

FIGURE 4: Temperature dependence of overall reaction heats for RMPK titrated with Phe. Cyan and red symbols represent data from ITC titrations in TKM and BTKM buffer, respectively. Lines represent the best global fits of all ITC data, i.e., all data from Figures 2−5.

an essentially temperature-independent heat of reaction for PEP binding. In contrast, there is an abrupt decrease in ΔH_{PEP}^{tot} above 30 °C. This significant change most likely reflects the contribution of heat due to the linked reaction of the RMPK conformation change. Since earlier work indicated that RMPK is present predominantly in the R state under these experimental conditions (*8*, *10*, *19*), a possible cause for the significant change in ΔH_{PEP}^{tot} is the conversion to the T state at these high temperatures and binding of PEP shifts RMPK back to the R state; i.e., the observed change could be assigned mainly to the R ↔ T transition. As the temperature increases, the fraction of the T state increases. Binding of PEP with a higher affinity to the R state shifts the R ↔ T equilibrium back toward the R state. Therefore, the heat of the R ↔ T transition is expected to be detected in addition to ligand binding heats (eq 1). The observed temperature dependence of ΔH_{PEP}^{tot} in Figure 3 is qualitatively in agreement with the behavior predicted by the two-state model.

The values of ΔH_{PEP}^{tot} are quite similar in two buffers with significantly different heats of ionization. This trend implies that PEP binding does not involve a change in proton release or absorption. Another possibility is that the changes in PEP binding and R ↔ T transition are similar in magnitude but opposite in sign, thus canceling the contribution of the other.

(*ii*) *Phe Binding*. ITC titration curves for Phe are depicted in Figure 4. In this case, the values of the heat of reaction increase with an increase in temperature. However, at 30 °C, the values

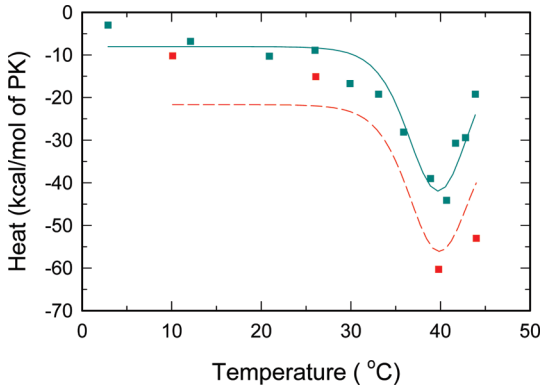

FIGURE 5: Temperature dependence of overall reaction heats for RMPK titrated with ADP. Cyan and red symbols represent data from ITC titrations in TKM and BTKM buffer, respectively. Lines represent the best global fits of all ITC data, i.e., all data from Figures 2−5.

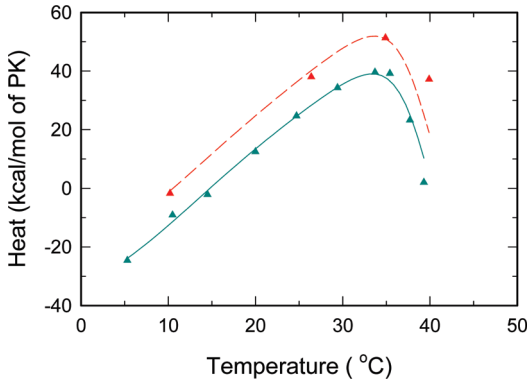

FIGURE 6: Overall reaction heats of RMPK titrated with Phe in the presence of 2 mM ADP. Cyan and red symbols represent data from ITC titrations in TKM and BTKM buffer, respectively. Lines represent the best global fits of all ITC data, i.e., all data from Figures 2−5. To avoid dilution artifacts, the same ADP concentration of 2 mM was present in the injectant during the ITC experiments.

decrease significantly with a further increase in temperature. Again, in this titration, only three linked reactions are involved, namely, R ↔ T conversion and binding of Phe to either of these states. The interaction with Phe is apparently analogous to the PEP−PK interaction. Similar thermal effects can be expected for binding of Phe that exhibits preferential binding to the T state (*8*, *10*, *19*). As the fraction of the T state decreases with the decrease in temperature, binding of Phe shifts the R ↔ T equilibrium back toward the T state. Because at a given temperature both PEP and Phe titrations start from the same distribution of states dictated by the R ↔ T equilibrium, similar (or complementary) curves are expected to be observed for the two ligands. Contrary to expectations, a plateau was not observed at low temperatures for the Phe titration. Instead, a positive slope of ΔH^{tot}_{Phe} is detected. Such data are not consistent with the model described by eqs 1−11; thus, some assumptions of the model have to be modified.

There are three possible causes for the observed effect. First, at low temperatures, the differential affinity of Phe for the R and T states is not sufficiently high to shift the R ↔ T equilibrium completely to the T state. Second, there is an isobaric heat capacity change ΔC_p involved in the binding of Phe or, third, in the R ↔ T transition.

To test for the first possibility, we modified the model and assumed an incomplete R ↔ T transition took place when RMPK was titrated with Phe. In particular, we assumed that ${}^{sat}f^{T}_{Phe} < 1$ in eq 1. However, the global analysis of the ITC data for PEP and Phe data from Figures 3 and 4 resulted in an unacceptably poor fit. This model is also in contradiction with published steady state kinetic data (*10*), and therefore, it was rejected. The second case was ruled out when a global fit of the data sets from Figures 3 and 4 completely failed (the program did not reach convergence) assuming a non-zero heat capacity change associated with Phe binding [$\Delta H^{T}_{Phe} = \Delta H^{T}_{0,Phe} + \Delta C^{T}_{p,Phe}(T - T_0)$].

To test for the third case, we incorporated into the model an isobaric heat capacity change $\Delta C_{p,R\leftrightarrow T}$ associated with the R ↔ T transition. In particular, we used the relationships $\Delta H_{R\leftrightarrow T} = \Delta H_{0,R\leftrightarrow T} + \Delta C_{p,R\leftrightarrow T}(T - T_0)$ and $\Delta S_{R\leftrightarrow T} = \Delta S_{0,R\leftrightarrow T} + \Delta C_{p,R\leftrightarrow T} \times \ln(T/T_0)$ for evaluation of L_0 in eq 10. With this model, we obtained a successful global fit of all curves from Figures 3 and 4.

The values of ΔH^{tot}_{Phe} are quite different in two buffers with significantly different heats of ionization. This trend implies that Phe binding involves a change in proton release or absorption.

(*iii*) *ADP Binding*. Figure 5 demonstrates the temperature dependence of thermal effects upon saturation of RMPK with ADP. A visual inspection of the figure reveals a pronounced minimum of the ΔH^{tot}_{ADP} curve above 35 °C. Interestingly, the sign of the dip agrees with the sign of ΔH^{tot}_{PEP} at high temperatures in Figure 3, where the R ↔ T transition is responsible for the major heat effects accompanying the PEP titration. On the basis of this observation, we suggest that above 30 °C the presence of ADP perturbs the R ↔ T equilibrium as a consequence of a differential affinity for the R and T states. Specifically, the presence of ADP seems to shift the R ↔ T equilibrium toward the R state. Consistent with published data (*8*, *10*, *19*), a flat region of ΔH^{tot}_{ADP} around room temperature indicates only minor shifts of the R ↔ T equilibrium induced by ADP binding. When curves from Figure 5 were included in the global data set, an excellent global fit of all six curves from Figures 3−5 was achieved with negligible changes in the parameters associated with the R ↔ T transition. This strongly supports our conclusion about $\Delta C_{p,R\leftrightarrow T}$ since all data sets are linked by the same R ↔ T equilibrium.

(*iv*) *Coupling between ADP and Phe Binding*. Having characterized RMPK behavior in the presence of single ligands, we repeated the Phe titrations in the presence of 2 mM ADP to evaluate possible interaction between ADP and Phe. The measured temperature dependence of $\Delta H^{tot}_{ADP,Phe}$ is shown in Figure 6. We found that $\Delta H^{tot}_{ADP,Phe}$ in the presence of ADP is significantly different from ΔH^{tot}_{Phe} shown in Figure 4. Although the shape of the curves seems to be similar, absolute values of the reaction heats differ and a maximum of $\Delta H^{tot}_{ADP,Phe}$ is located at a higher temperature compared to that of ΔH^{tot}_{Phe}. When curves from Figure 6 were included in the global data set assuming that there is no interaction between the binding sites for ADP and Phe, the quality of the global fit significantly degraded which invalidated our assumption about the noninteracting sites for these ligands. On the basis of the fitting results, as well as independent evidence of the ADP−Phe interaction gleened from florescence data (DOI: 10.1021/bi900280u), we introduced an interaction enthalpy term, $\Delta\Delta H^{T}_{ADP,Phe}$, and an interaction entropy term, $\Delta\Delta S^{T}_{ADP,Phe}$, for binding of Phe to the T state in the presence of ADP:

$$\Delta H^{T}_{ADP,Phe} = \Delta H^{T}_{Phe} + \Delta\Delta H^{T}_{ADP,Phe} \quad (12)$$

$$\Delta S^{T}_{ADP,Phe} = \Delta S^{T}_{Phe} + \Delta\Delta S^{T}_{ADP,Phe} \quad (13)$$

Table 1: Parameters Obtained by Global Fitting of the ITC Data

reaction	parameter	value	unit[a]
R ↔ T	$\Delta S_{0,R\rightarrow T}$	152 (6)[c,e]	cal mol^{-1} K^{-1}[b]
	$\Delta H_{0,R\rightarrow T}$	48 (10)[c]	kcal mol^{-1}[b]
	$\Delta C_{p,R\rightarrow T}$	2.2 (0.2)[c]	kcal mol^{-1} K^{-1}[b]
	$\Delta n_{R\rightarrow T}$	0.5 (0.3)[d,f]	mol^{-1}[b]
Phe binding	ΔS^{R}_{Phe}	7 (5)	cal mol^{-1} K^{-1}
	ΔH^{R}_{Phe}	0.9 (2.0)	kcal mol^{-1}
	ΔS^{T}_{Phe}	13 (7)[g]	cal mol^{-1} K^{-1}
	ΔH^{T}_{Phe}	0.8 (1.0)	kcal mol^{-1}
	Δn^{T}_{Phe}	−0.9 (0.1)[f]	mol^{-1}[b]
PEP binding	ΔH^{R}_{PEP}	−2.1 (0.8)	kcal mol^{-1}
	Δn^{R}_{PEP}	0.18 (0.03)[f]	mol^{-1}[b]
ADP binding	ΔS^{R}_{ADP}	−20 (2)	cal mol^{-1} K^{-1}
	ΔH^{R}_{ADP}	−10.3 (1.0)	kcal mol^{-1}
	Δn^{R}_{ADP}	0.74 (0.06)	
	ΔS^{T}_{ADP}	−29 (3)	cal mol^{-1} K^{-1}
	ΔH^{T}_{ADP}	−13 (2)	kcal mol^{-1}
	Δn^{T}_{ADP}	1.00 (0.02)[f]	mol^{-1}[b]
ADP−Phe coupling	$\Delta\Delta S^{T}_{ADP,Phe}$	−2.5 (2.0)	cal mol^{-1} K^{-1}
	$\Delta\Delta H^{T}_{ADP,Phe}$	−0.46 (0.30)	kcal mol^{-1}
	$\Delta n^{R}_{ADP,Phe}$	−1.7 (1.0)[f]	mol^{-1}[b]

[a]Per mole of ligand. [b]Per mole of tetramer. [c]For T_0 = 20 °C. T_0 was a fixed parameter. [d]Buffer ionization heats of 11.3 and 6.8 kcal/mol for TKM and BTKM, respectively (*38*). [e]Estimated deviations from multiple fittings. [f]Number of protons absorbed. [g]This value was taken from the limited global fitting of the ITC and the fluorescence data.

The described modification renders dissociation constant $K^{T}_{ADP,Phe}$ independent of K^{T}_{Phe}. However, because of the interaction, we can no longer assume that PK saturated with Phe is always in the T state, irrespective of temperature and ADP concentration. The full eq 1 was used for calculation of the reaction heats. After the model modification, the global fit of all eight curves from Figures 3−6 dramatically improved.

(*v*) *RMPK Conformation Change*. The best global fit is shown in Figures 3−6 by solid and dashed lines. Fitted parameters are summarized in Table 1. The R ↔ T concerted conformational transition is strongly entropy-driven with a significant entropy term of 152 cal K^{-1} (mol of enzyme)$^{-1}$. The transition also involves a fairly large enthalpy change of 48 kcal/mol of PK. Such large values indicate a strong temperature dependence of the equilibrium between the active and inactive state. Moreover, the heat capacity change of 2.2 kcal K^{-1} (mol of enzyme)$^{-1}$ associated with the transition causes L_0 to deviate from a monotonic dependence on temperature. The minimum of L_0, where RMPK is mostly in the active R state, was found to be located near −3 °C.

DISCUSSION

We were cognizant that the multidimensional χ^2 surface could contain local minima. To avoid being trapped in such minima, the global fitting procedure was initiated with data from a subset of curves only. Then data from additional curves were individually added. This was followed by a subsequent optimization of parameters until all data sets were included. This procedure was repeated by initiating the analysis process with several different sets of data and expanding the database by adding different data sets in different orders. Identical final values were derived for the same parameter regardless of the specific order of data that was included in the analysis procedure; thus, we are confident that the reported values for these parameters represent the global minima. The global fitting was also initiated from different starting estimated values for these parameters to ensure that the fitting converges to the same global χ^2 minimum.

The results of this in-depth dissection of the thermodynamic signatures of RMPK interacting with metabolites provide novel insights into the mechanism of allosteric regulation of RMPK.

1. The state of RMPK that ADP preferentially binds is temperature-dependent. ADP binds more favorably to the T and R states at high and low temperatures, respectively. This crossover of affinity toward the R and T states implies that ADP not only serves as a substrate but also plays an important and intricate role in regulating RMPK activity.
2. The binding of Phe is negatively coupled to that of ADP in addition to the shifting of the R ↔ T equilibrium due to the relative affinities of Phe or ADP for these two states; i.e., the assumption that ligand binding to RMPK is state-dependent is only correct for PEP but not Phe or ADP.
3. The release or absorption of protons linked to the various equilibria is specific to the particular reaction. As a consequence, pH will exert a complex effect on these linked equilibria, with the net effect being manifested in the regulatory behavior of RMPK.
4. The R ↔ T equilibrium is accompanied by a significant ΔC_p.

Binding of ADP to both states of RMPK was found to be strongly enthalpy-driven with binding enthalpies to the R and T states of approximately −10 and −13 kcal/mol, respectively. This is consistent with a binding mechanism that involves electrostatic interaction with the highly charged ADP substrate. Both entropy and enthalpy changes for binding of ADP were found to be the largest among all investigated ligands. ADP binding and the differential affinity toward the R and T states exhibit a pronounced temperature dependence. The affinity for the T state is stronger at elevated temperatures. As a consequence, at high temperatures ADP binds more favorably to the T state, which results in a shift of the R ↔ T equilibrium toward the inactive T state; thus, in this particular regard, ADP behaves like an inhibitor at high temperatures. However, by virtue of its chemical structure, ADP is still a substrate of RMPK. In earlier studies, it was concluded that ADP behaves strictly as a substrate which plays a minor role in the allosteric regulation of RMPK because it does not show any differential affinity toward the two states of RMPK. However, as a consequence of extending the temperature range in this study, we revealed that ADP actually plays a major role in the allosteric mechanism in RMPK at physiologically relevant temperatures.

Phenylalanine binding in the presence of ADP revealed that an antagonism exists between the two ligands; i.e., Phe was found to bind more weakly in the presence of ADP. Table 1 indicates that due to the interaction enthalpy, $\Delta\Delta H^{T}_{ADP,Phe}$, of approximately −0.5 kcal/mol, the enthalpy term $\Delta H^{T}_{ADP,Phe} = \Delta H^{T}_{Phe} + \Delta\Delta H^{T}_{ADP,Phe}$ is reduced almost to zero. Concomitantly, the entropy change, $\Delta S^{T}_{ADP,Phe} = \Delta S^{T}_{Phe} + \Delta\Delta S^{T}_{ADP,Phe}$ becomes smaller by 2.5 cal mol^{-1} K^{-1}. The net consequence of the coupling between ADP and Phe bindings is a reduction in the enthalpy term for Phe binding to essentially zero and a less favorable entropy term; i.e., the presence of a bound ADP exerts a negative effect on binding of Phe to the T state. Thus, at high but

physiologically relevant temperatures, the bound ADP modulates the inhibitory efficiency of Phe by reducing its affinity for the T state.

Information related to linked proton reactions associated with ligand binding and the state transition is also available from Table 1. The following reactions summarize these results:

reactions with proton absorption

$$0.2H^+ + PEP + R \leftrightarrows PEP\cdot R; \quad 0.5H^+ + R \leftrightarrows T$$

$$0.7H^+ + ADP + R \leftrightarrows ADP\cdot R; \quad 1.0H^+ + ADP + T \leftrightarrows ADP\cdot T$$

reactions with proton release

$$Phe + T \leftrightarrows Phe\cdot T + 0.9H^+$$

$$ADP + Phe + T \leftrightarrows ADP\cdot Phe\cdot T + 1.7H^+$$

Binding of substrates apparently always absorb protons, although the binding of ADP involves a larger amount of protons absorbed. Consequently, the binding of ADP would be more sensitive to pH perturbations. The R → T transition would also absorb protons. For the reactions that involve proton absorption, a lower pH would shift the equilibria to the right, as defined by Le Chatelier's principle. Thus, a lower pH would favor the bindings of ADP, PEP, and the T state. The net result would be an expected change in cooperativity in substrate binding, the extent of which is pH-dependent.

In contrast, binding of Phe to the T state, in the presence or absence of ADP, leads to release of protons. Another significant observation is that the amount of protons released almost doubles in the presence of ADP. If the bindings of Phe and ADP were simply a summation of the two reactions (absorption of 0.7 H^+ and release of 0.9 H^+ for ADP and Phe binding, respectively), then the net amount of proton release is expected to be approximately zero; instead, the observation is a doubling of the number of H^+ released to 1.7. This is a clear indication of the coupling of the two binding events. Binding of Phe and ADP to the T state seems to be more pH-dependent.

These results clearly indicate that the effect of pH on the basic allosteric behavior of RMPK is a composite of the nature and magnitude of proton release or absorption linked to the various reactions. According to Wyman's linked-function theory (*36*), there should be dependence of dissociation constants on a concentration of protons and shift of the R ↔ T equilibrium. For example, at low pH, the T state is favored but the binding of Phe would be weakened. Thus, a binding isotherm of Phe is pH-dependent as a function of the relative values of equilibrium constants that define the distribution of the R and T state and the relative affinities of Phe for these states. Simultaneously, the affinity of substrates would be affected. Thus, one should expect that the allosteric behavior of RMPK is a complex phenomenon defined by the specific experimental conditions. It is most gratifying to note that such an expectation was reported in 1990 by Consler et al.(*19*). On the basis of steady state kinetic studies, these authors reported the synergistic effects of protons and Phe on the regulation of RMPK.

The kinetic results (*10*) are consistent with our study which shows that binding of Phe was found to be entropy-driven with the entropy term, ΔS^T_{Phe}, for binding to the T state being approximately twice as large as the entropy change for binding to the R state, ΔS^R_{Phe}. These results imply that the binding of Phe is driven mainly by hydrophobic interactions that generally strengthen with an increase in temperature and Phe binds more favorably to the T state. Relatively small and similar values of the enthalpy changes ($\Delta H^R_{Phe} = 0.9$ kcal/mol and $\Delta H^T_{Phe} = 0.8$ kca/mol for binding of Phe to the R and T states, respectively) indicate an only weak dependence of the binding constants on temperature. Calorimetric data revealed that binding of the PEP substrate to the active R conformation of the enzyme involves an enthalpy change ΔH^R_{PEP} of −2.1 kcal/mol. The entropy change, ΔS^R_{PEP}, as well as parameters characterizing binding of PEP to the T state were not accessible from our data primarily because in the absence of ligands the equilibrium for the conformation state of RMPK is heavily in favor of the R state. Since PEP binds very favorably to the R state, the binding to the T state most likely is not enthaly-driven. As a consequence, no parameters associated with binding of PEP to the T state can be defined with confidence.

The significant ΔC_p detected in the R ↔ T transition is consistent with the report of dynamic movement of the B domain with respect to the rest of the molecule as detected by small-angle neutron scattering in conjunction with molecular modeling (*21*). This domain movement can be modulated by mutation as detected by X-ray crystallography in S402P RMPK (*37*).

Our conclusions derived from calorimetric data are in full agreement with those based on our published steady state kinetic studies. These conclusions are further strengthened by our fluorescence data and model simulations described in the following two papers of this issue (DOI: 10.1021/bi900280u and 10.1021/bi900281s).

ACKNOWLEDGMENT

We thank Drs. X. Cheng and A. Gribenko for critical review of the manuscript. This series of papers is dedicated to Professor Serge N. Timasheff who taught us the beauty and power of thermodynamics of linked reactions in biology.

REFERENCES

1. Pawson, T., and Nash, P. (2003) Assembly of cell regulatory systems through protein interaction domains. *Science 300*, 445–452.
2. Copley, R. R., and Bork, P. (2000) Homology among $(\beta\alpha)_8$ barrels: Implications for the evolution of metabolic pathways. *J. Mol. Biol. 303*, 627–640.
3. Heggi, H., and Gerstein, M. (1999) The relationship between protein structure and function: A comprehensive survey with application to the yeast genome. *J. Mol. Biol. 288*, 147–164.
4. Williams, R., Holyoak, T., McDonald, G., Gui, C., and Fenton, A. W. (2006) Differentiating a ligand's chemical requirements for allosteric interactions from those for protein binding. Phenylalanine inhibition of pyruvate kinase. *Biochemistry 45*, 5421–5429.
5. Dombrauckas, J. D., Santarsiero, B. D., and Mesecar, A. D. (2005) Structural basis for tumor pyruvate kinase M2 allosteric regulation and catalysis. *Biochemistry 44*, 9417–9429.
6. Ainsworth, S., and MacFarlane, N. (1973) A kinetic study of rabbit muscle pyruvate kinase. *Biochem. J. 131*, 223–236.
7. Hall, E. R., and Cottam, G. L. (1978) Isozymes of pyruvate kinase in vertebrates: Their physical, chemical, kinetic and immunological properties. *Int. J. Biochem. 9*, 785–793.
8. Oberfelder, R. W., Barisas, B. G., and Lee, J. C. (1984) Thermodynamic linkages in rabbit muscle pyruvate kinase: Analysis of experimental data by a two-state model. *Biochemistry 23*, 3822–3826.
9. Consler, T. G., Woodard, S. H., and Lee, J. C. (1989) Effects of primary sequence differences on the global structure and function of an enzyme: A study of pyruvate kinase isozymes. *Biochemistry 28*, 8756–8764.
10. Consler, T. G., Jennewein, M. J., Cai, G. Z., and Lee, J. C. (1992) Energetics of Allosteric Regulation in Muscle Pyruvate Kinase. *Biochemistry 31*, 7870–7878.
11. Larsen, T. M., Laughlin, L. T., Holden, H. M., Rayment, I., and Reed, G. H. (1994) Structure of rabbit muscle pyruvate kinase

complexed with Mn^{2+}, K^+, and pyruvate. *Biochemistry 33*, 6301–6309.
12. Boyer, P. D. (1962) in The Enzymes (Boyer, P. D., Lardy, H., and Myrback, K., Eds.) Vol. 6, p 95, Academic Press, New York.
13. Carminatti, H., Jimenez de Asua, L., Leiderman, B., and Rozengurt, E. (1971) Allosteric properties of skeletal muscle pyruvate kinase. *J. Biol. Chem. 246*, 7284–7288.
14. Kayne, F. J., and Price, N. C. (1972) Conformational changes in the allosteric inhibition of muscle pyruvate kinase by phenylalanine. *Biochemistry 11*, 4415–4420.
15. Kayne, F. J., and Price, N. C. (1973) Amino acid effector binding to rabbit muscle pyruvate kinase. *Arch. Biochem. Biophys. 159*, 292–296.
16. Kwan, C. Y., and Davis, R. C. (1980) pH-dependent amino acid induced conformational changes of rabbit muscle pyruvate kinase. *Can. J. Biochem. 58*, 188–193.
17. Kwan, C. Y., and Davis, R. C. (1981) L-Phenylalanine induced changes of sulfhydryl reactivity in rabbit muscle pyruvate kinase. *Can. J. Biochem. 59*, 92–99.
18. Oberfelder, R. W., Lee, L. L., and Lee, J. C. (1984) Thermodynamic linkages in rabbit muscle pyruvate kinase: Kinetic, equilibrium, and structural studies. *Biochemistry 23*, 3813–3821.
19. Consler, T. G., Jennewein, M. J., Cai, G. Z., and Lee, J. C. (1990) Synergistic effects of proton and phenylalanine on the regulation of muscle pyruvate kinase. *Biochemistry 29*, 10765–10771.
20. Consler, T. G., and Lee, J. C. (1988) Domain interaction in rabbit muscle pyruvate kinase. I. Effects of ligands on protein denaturation induced by guanidine hydrochloride. *J. Biol. Chem. 263*, 2787–2793.
21. Consler, T. G., Uberbacher, E. C., Bunick, G. J., Liebman, M. N., and Lee, J. C. (1988) Domain interaction in rabbit muscle pyruvate kinase. II. Small angle neutron scattering and computer simulation. *J. Biol. Chem. 263*, 2794–2801.
22. Heyduk, E., Heyduk, T., and Lee, J. C. (1992) Global conformational changes in allosteric proteins. A study of *Escherichia coli* cAMP receptor protein and muscle pyruvate kinase. *J. Biol. Chem. 267*, 3200–3204.
23. Monod, J., Wyman, J., and Changeux, J. P. (1965) On the Nature of Allosteric Transitions: A Plausible Model. *J. Mol. Biol. 12*, 88–118.
24. Yu, S., Lee, L. L., and Lee, J. C. (2003) Effects of metabolites on the structural dynamics of rabbit muscle pyruvate kinase. *Biophys. Chem. 103*, 1–11.
25. Knutson, J. R., Beechem, J. M., and Brand, L. (1983) Simultaneous Analysis of Multiple Fluorescence Decay Curves: A Global Approach. *Chem. Phys. Lett. 102*, 501–507.
26. Beechem, J. M., Knutson, J. R., Ross, J. B. A., Turner, B. W., and Brand, L. (1983) Global Resolution of Heterogeneous Decay by Phase Modulation Fluorometry: Mixtures and Proteins. *Biochemistry 22*, 6054–6058.
27. Bevington, P. R., and Robinson, D. K. (2002) Data reduction and error analysis for the physical sciences , 3rd ed., McGraw-Hill, New York.
28. Eisenfeld, J., and Ford, C. C. (1979) A systems-theory approach to the analysis of multiexponential fluorescence decay. *Biophys. J. 26*, 73–83.
29. Beechem, J. M., Ameloot, M., and Brand, L. (1985) Global and target analysis of complex decay phenomena. *Anal. Instrum. 14*, 379–402.
30. Boo, B. H., and Kang, D. (2005) Global and target analysis of time-resolved fluorescence spectra of di-9H-fluoren-9-yldimethylsilane: Dynamics and energetics for intramolecular excimer formation. *J. Phys. Chem. A 109*, 4280–4284.
31. Ionescu, R. M., and Eftink, M. R. (1997) Global analysis of the acid-induced and urea-induced unfolding of staphylococcal nuclease and two of its variants. *Biochemistry 36*, 1129–1140.
32. Ucci, J. W., and Cole, J. L. (2004) Global analysis of non-specific protein-nucleic interactions by sedimentation equilibrium. *Biophys. Chem. 108*, 127–140.
33. Vermunicht, G., Boens, N., and de Schryver, F. C. (1991) Global analysis of the time-resolved fluorescence of α-chymotrypsinogen A and α-chymotrypsin powders as a function of hydration. *Photochem. Photobiol. 53*, 57–63.
34. Verveer, P. J., Squire, A., and Bastiaens, P. I. (2000) Global analysis of fluorescence lifetime imaging microscopy data. *Biophys. J. 78*, 2127–2137.
35. Marquardt, D. W. (1963) An Algorithm for Least-Squares Estimation of Nonlinear Parameters. *J. Soc. Ind. Appl. Math. 11*, 431–441.
36. Wyman, J., Jr. (1964) Linked Functions and Reciprocal Effects in Hemoglobin: A Second Look. *Adv. Protein Chem. 19*, 223–286.
37. Wooll, J. O., Friesen, R. H. E., White, M. A., Watowich, S. J., Fox, R. O., Lee, J. C., and Czerwinski, E. W. (2001) Structural and Functional Linkages Between Subunit Interfaces in Mammaliam Pyruvate Kinase. *J. Mol. Biol. 312*, 525–540.
38. Christensen, J. J., Hansen, L. D., and Reed, M. I. (1976) Handbook of Proton Ionization Heats and Related Thermodynamic Quantities, John Willey & Sons, New York.